

# State-of-the-Art Review

## First-trimester fetal neurosonography: technique and diagnostic potential

N. VOLPE<sup>1</sup>, A. DALL'ASTA<sup>1</sup>,  
 E. DI PASQUO<sup>1</sup>, T. FRUSCA and T. GHI\*<sup>1</sup>

Department of Medicine and Surgery, Unit of Surgical Sciences, Obstetrics and Gynecology, University of Parma, Parma, Italy  
 \*Correspondence. (e-mail: tullioghi@yahoo.com)

### ABSTRACT

*Most brain abnormalities are present in the first trimester, but only a few are detected so early in gestation. According to current recommendations for first-trimester ultrasound, the fetal head structures that should be visualized are limited to the cranial bones, the midline falx and the choroid-plexus-filled ventricles. Using this basic approach, almost all cases of acrania, alobar holoprosencephaly and cephalocele are detected. However, the majority of other fetal brain abnormalities remain undiagnosed until the midtrimester. Such anomalies would be potentially detectable if the sonographic study were to be extended to include additional anatomic details not currently included in existing guidelines. The aim of this review article is to describe how best to assess the normal fetal brain by first-trimester expert multiplanar neurosonography and to demonstrate the early sonographic findings that characterize some major fetal brain abnormalities. © 2020 International Society of Ultrasound in Obstetrics and Gynecology.*

### INTRODUCTION

Fetal brain abnormalities are among the most common congenital malformations, with a reported prevalence in Europe of about 1 per 1000 births<sup>1</sup>. According to the area of the brain involved and the type of abnormality, the prognosis is mostly poor, with a substantial impact on both neurodevelopmental and cognitive outcome. The sensitivity of prenatal ultrasound for detection of central nervous system (CNS) congenital malformations ranges between 68% and 92%<sup>2,3</sup>, but a comprehensive evaluation and diagnosis of the defect is usually difficult on standard examination. While fetal CNS defects are usually suspected at the screening ultrasound evaluation, an expert multiplanar examination is required for an accurate diagnosis and classification of each brain anomaly. The multiplanar fetal neurosonogram is usually performed at

around 20 weeks' gestation or later, and its methodology has been described by the International Society of Ultrasound in Obstetrics and Gynecology (ISUOG)<sup>4</sup>.

Most brain abnormalities are in fact present in the first trimester, but only a few are detected so early in gestation<sup>5–14</sup>. According to the current ISUOG recommendations for the first-trimester scan<sup>15</sup>, the fetal head structures that should be visualized are limited to the cranial bones, the midline falx and the choroid-plexus-filled ventricles. Using this basic approach, almost all cases of acrania, alobar holoprosencephaly and cephalocele are detected<sup>6–8,10,13</sup>, while the majority of other brain abnormalities remain undiagnosed until the midtrimester. The low detection rates of brain abnormalities in the first trimester could be related to the small size of the fetal brain structures as well as to the fact that some develop only later in pregnancy. Moreover, in the first trimester, some brain abnormalities do not affect the sonographic appearance of the basic intracranial structures whose examination is suggested at this stage. Most of these anomalies are potentially detectable, but only if the sonographic study is extended to include anatomic details which are not currently specified in first-trimester guidelines. Indeed, only a detailed knowledge of the normal sonographic appearance of the fetal brain in the first trimester allows recognition of the early anatomic modifications which herald the typical appearance of major cerebral abnormalities in the second trimester, when their sonographic findings are more widely recognized. For some brain malformations, such as severe ventriculomegaly, callosal agenesis, cranial posterior fossa (CPF) anomalies and Chiari-II anomaly, the sonographic appearance is considerably different at 12 weeks compared with that in the second trimester and they are suspected in the first trimester only if particular ultrasonographic landmarks are assessed by an expert eye.

In recent years, high-resolution ultrasound machines have provided the opportunity to evaluate the subtle details of fetal anatomy earlier in gestation and to improve our understanding of the normal and abnormal sonoembryological development of the fetal brain. Studies on the development of the fetal brain during the first weeks of pregnancy have characterized the developing brain structures using H-thymidine labeling<sup>16</sup> of anatomic specimens. Thanks to these studies, good correlation between high-resolution sonographic images and anatomic findings may be achieved.

The aims of this review article are two-fold: to describe how best to assess the normal fetal brain by first-trimester expert multiplanar neurosonography and to demonstrate the early sonographic findings that characterize some major fetal brain abnormalities.

## NORMAL FIRST-TRIMESTER FETAL BRAIN ANATOMY

### Axial views

Approaching the 11 + 0 to 13 + 6-week fetal brain using axial views, it is possible to evaluate its sonographic appearance in two different anatomical planes: a plane just above the third ventricle and thalami (Figure 1: supratheralamic section) and a plane at the level of the thalami (Figure 2: transthalamic section). These two planes are obtained when the ultrasound beam is oriented perpendicular to the midline echo.

The supratheralamic view represents the most common scanning plane obtained in the first trimester, and allows evaluation of the interhemispheric fissure (midline echo), the lateral ventricles, containing their choroid plexuses,

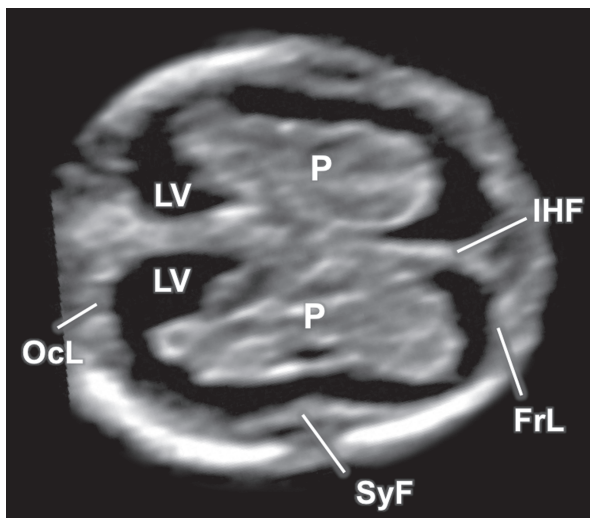


**Figure 1** Axial view (supratheralamic section) on two-dimensional ultrasound imaging in normal 11–13-week fetus. FrL, frontal lobe cortex; IHF, interhemispheric fissure; LV, lateral ventricle; OcL, occipital lobe cortex; P, choroid plexus; SyF, future Sylvian fissure.

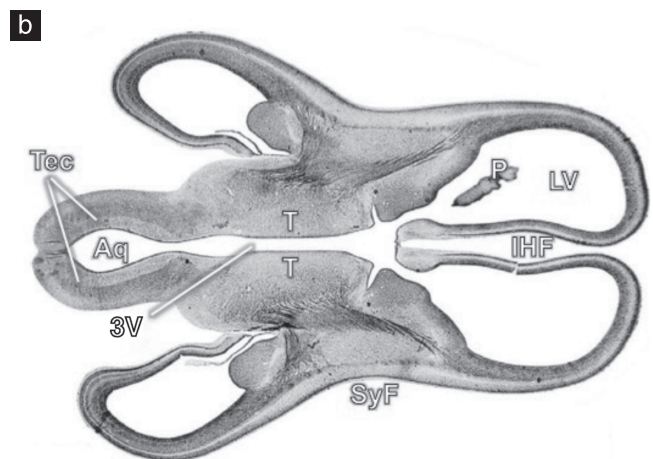
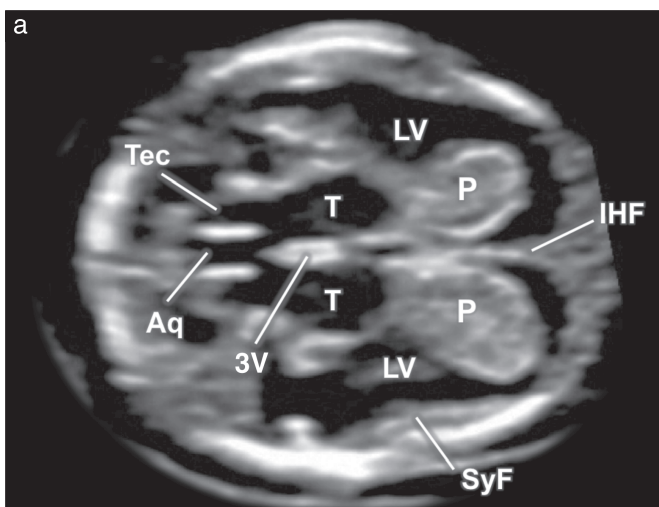


**Figure 2** Axial view (transthalamic section) on two-dimensional ultrasound imaging in normal 11–13-week fetus (a) and corresponding anatomic specimen (b). 3V, third ventricle; Aq, aqueduct of Sylvius; IHF, interhemispheric fissure; LV, lateral ventricle; P, choroid plexus; SyF, future Sylvian fissure; T, thalamus; Tec, tectum. Anatomic specimen reproduced from Bayer and Altman<sup>16</sup> with permission.

the rudimentary cortex and the surrounding calvarium (Figure 1). At this early stage, the calvarium shape, integrity and calcification can be assessed; the absence of intact cranial bones surrounding the brain can be a sign of acrania or other neural tube defects<sup>17,18</sup>. The midline echo should be seen as a straight, uninterrupted hyperechoic line, dividing the brain into two equal symmetric parts. Any interruption of the midline echo should be noted, as this could be suggestive of alobar holoprosencephaly. On both sides of the cerebral midline are seen the two lateral ventricles, each occupied almost entirely by its choroid plexus. The two choroid plexuses are expected to be similar in size and symmetric in terms of shape and position, giving an overall appearance that resembles a butterfly<sup>19</sup>. The rudimentary surrounding cortex seems not to show any fissure or gyri at this stage, with the exception of the mild lateral recess, which represents the future Sylvian fissure.

Sweeping the transducer more caudally, the transthalamic view (Figure 2) is obtained as a slightly oblique head section, with the third ventricle, then the thalami and finally the aqueduct of Sylvius being visualized (Figure 2). In this view, only the anterior third of the midline echo is visible, being interrupted posteriorly by the third ventricle. The latter structure appears as a thin, anechoic space, between the two thalami. On prenatal ultrasound, the thalami appear as two separate, symmetrical, anechoic ovoid structures and, posterior to them, on the midline, it is possible to visualize the aqueduct of Sylvius as an anechoic rectangle-shaped cavity, lined by the anechoic tectum on either side.

### Sagittal views

Since the initial publications, more than 25 years ago<sup>20,21</sup>, on the clinical usefulness of nuchal translucency (NT) measurement on first-trimester screening for fetal chromosomal abnormalities, the acquisition of the midsagittal

view of the fetal head in the first trimester has become widely used. This is the only scanning plane in which the NT thickness can be measured properly, following strict methodological criteria that ensure high accuracy, reproducibility and repeatability of the measurement. In order to obtain the midsagittal view of the fetal head at 11–13 weeks, the ultrasound beam should be aligned with the midsagittal suture from the direction of the anterior fontanel<sup>15,22</sup>. In this scanning plane, in addition

to NT measurement, a thorough sonographic assessment of the midline cerebral structures can be performed. The diencephalon is visible as a hypoechoic, round structure. Caudal to this is the brainstem (BS), which includes the mesencephalon, the pons and the medulla (Figure 3). The BS has a typical ‘S’ shape due to the mesencephalic and pontine flexures. Behind the BS, within the CPF, it is possible to visualize the fourth ventricle (4V, also referred to as the ‘intracranial translucency’) and the

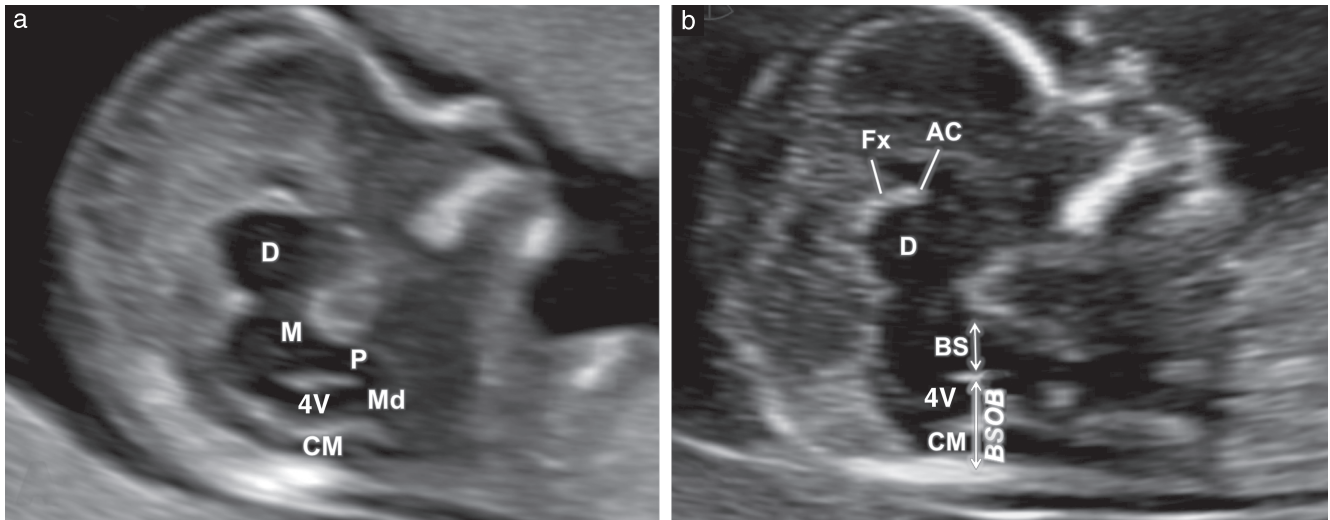


**Figure 3** Midsagittal view (frontal approach) of normal fetal brain on two-dimensional ultrasound imaging at 11–13 weeks, showing: (a) detailed anatomy of cranial posterior fossa and (b) measurements of posterior fossa structures and detailed anatomy of visible midline structures. 4V, fourth ventricle; AC, anterior commissure; BS, brainstem; BSOB, brainstem-to-occipital bone distance; CM, cisterna magna; D, diencephalon; Fx, fornix; M, mesencephalon; Md, medulla; P, pons.

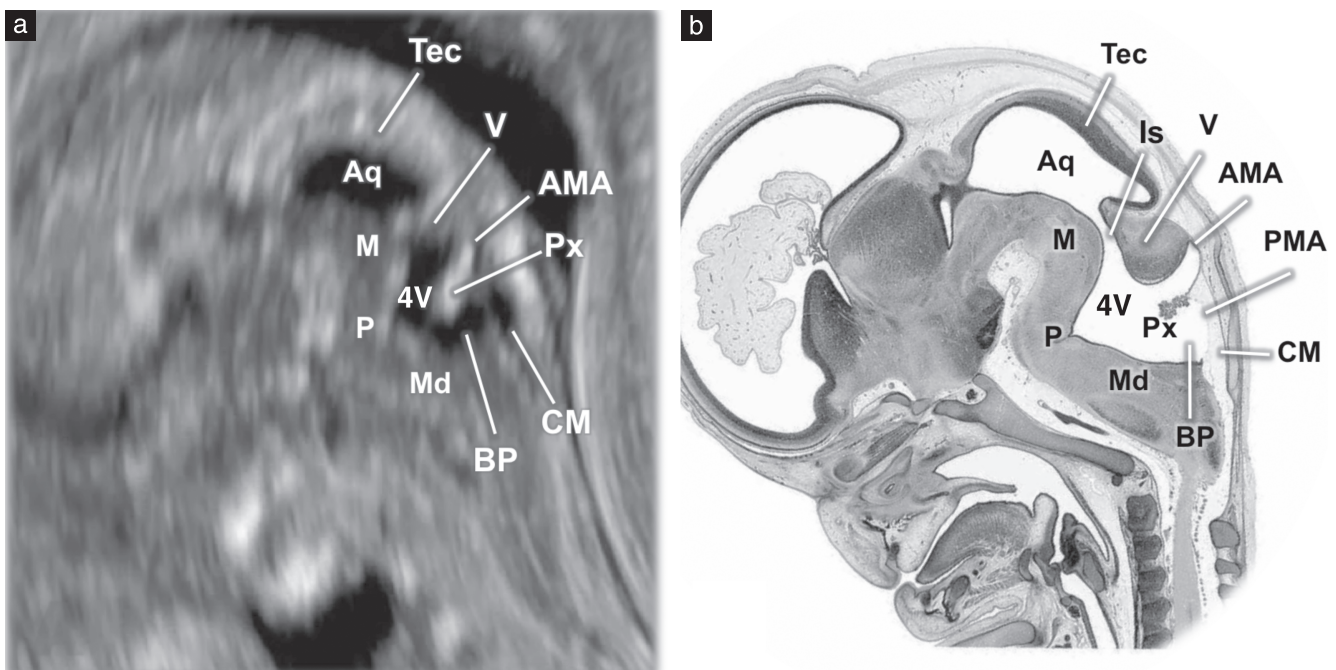


**Figure 4** Midsagittal view (posterior approach) of normal fetal brain, showing: (a) detailed anatomy of cranial posterior fossa and aqueduct of Sylvius (Aq) on two-dimensional ultrasound imaging at 11–13 weeks and (b) corresponding anatomic specimen. 4V, fourth ventricle; AMA, anterior membranous area; BP, Blake's pouch; CM, cisterna magna; Is, isthmus; M, mesencephalon; Md, medulla; P, pons; PMA, posterior membranous area; Px, plexus of fourth ventricle; Tec, tectum; V, cerebellar vermis. Anatomic specimen reproduced from Bayer and Altman<sup>16</sup> with permission.

cisterna magna (CM), these three structures (BS, 4V and CM) forming three parallel anechoic spaces between the sphenoid bone and the occipital bone<sup>23</sup>. Under normal circumstances, the ratio between the BS thickness and its distance to the occipital bone is 0.5–1.0<sup>24,25</sup>. Above the diencephalon, it is possible to distinguish the fornix, as a thin, hyperechoic line, whose cranial extremity is slightly thickened and forms the anterior commissure (Figure 3).

When approaching the fetal head in the midsagittal plane posteriorly, through the posterior fontanel, a comprehensive view of the posterior cerebral structures can be obtained. In this view, the subtle anatomic details of the developing BS and CPF can be demonstrated<sup>16,26–28</sup>. The aqueduct of Sylvius and the 4V can be visualized as anechoic spaces behind the BS, separated by the isthmus at the level of the mesencephalic flexure (Figure 4). At the end of the first trimester, the aqueduct is larger than it is in the second trimester, with a size similar to that of the 4V and an elongated shape, and is roofed by the tectum. The 4V sits behind the BS, mainly within its pontine flexure. The roof of the 4V is a medullary velum divided into two parts by the choroid plexus of the ventricle, which protrudes into the middle. Above the plexus, the velum is defined as the anterior membranous area, which is in continuity with the cerebellar vermis at its upper extremity. Below the choroid plexus, the velum is defined as the posterior membranous area, protruding into the CM as a finger-shaped structure, Blake’s pouch. Sonographic demonstration of some of these structures, along with their development and measurement, has been reported recently<sup>28,29</sup>.

**Coronal views**

Aligning the ultrasound beam perpendicularly to the sagittal suture, a parallel sweep of the probe, from the forehead to the occiput, obtains, in sequence, the

coronal planes of the fetal brain: the frontal, transcaudate, transthalamic and occipital planes (Figure 5).

The frontal view, passing through the frontal horns of the developing lateral ventricles, displays the anterior part of the corresponding choroid plexuses on either side of the interhemispheric fissure (Figure 6). Just below the

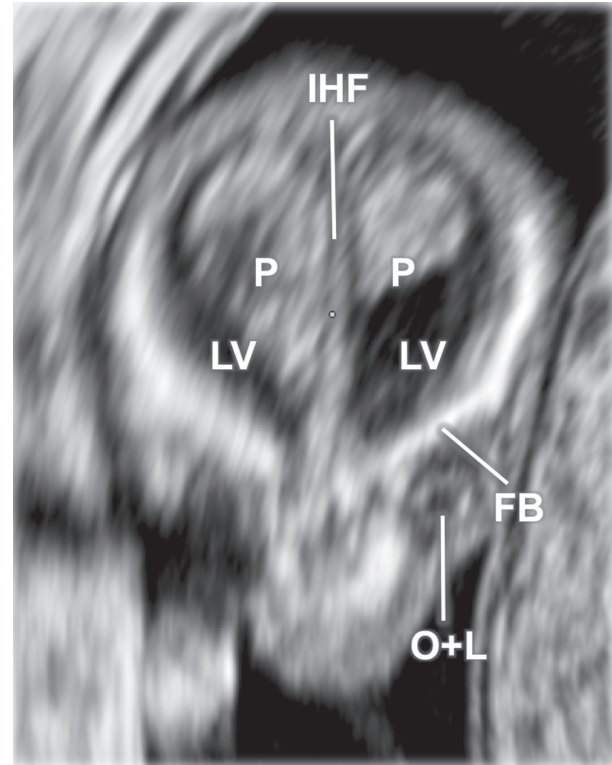


**Figure 6** Frontal coronal view of normal fetal brain on two-dimensional ultrasound imaging at 11–13 weeks. FB, frontal bone; IHF, interhemispheric fissure; LV, lateral ventricle; O+L, eye orbit and lens; P, choroid plexus.

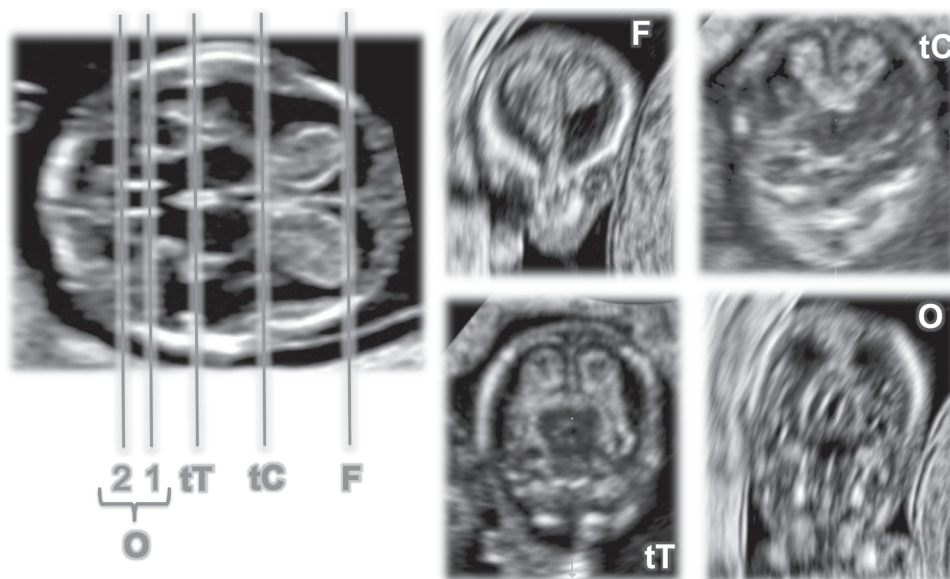


**Figure 5** Coronal views of normal fetal brain on two-dimensional ultrasound imaging at 11–13 weeks: frontal (F), transcaudate (tC), transthalamic (tT) and occipital (O) planes.

brain, in this plane, it is possible to visualize the fetal orbits with the lenses.

In the transcaudate view, the lateral ventricles with their choroid plexuses on either side of the interhemispheric fissure, the ganglionic eminences at the bases of the lateral ventricles and the basal ganglia (including the caudate) below them can be seen. Between the basal ganglia it is possible to visualize the third ventricle (Figure 7).

In the transthalamic view, the thalami are seen, appearing as round symmetric structures with low

echogenicity. The two lateral ventricles are also visible in this plane. Between the thalami, it is possible to visualize the caudal portion of the third ventricle (Figure 8).

Finally, in the occipital view, the posterior horns of the lateral ventricles are depicted, together with the aqueduct just below them, on the midline, and the two rudimentary cerebellar hemispheres on either side of the midline. The upper portion of the aqueduct is surrounded by the tectum, and its lower portion by the isthmus. It is possible to distinguish two occipital coronal planes, a

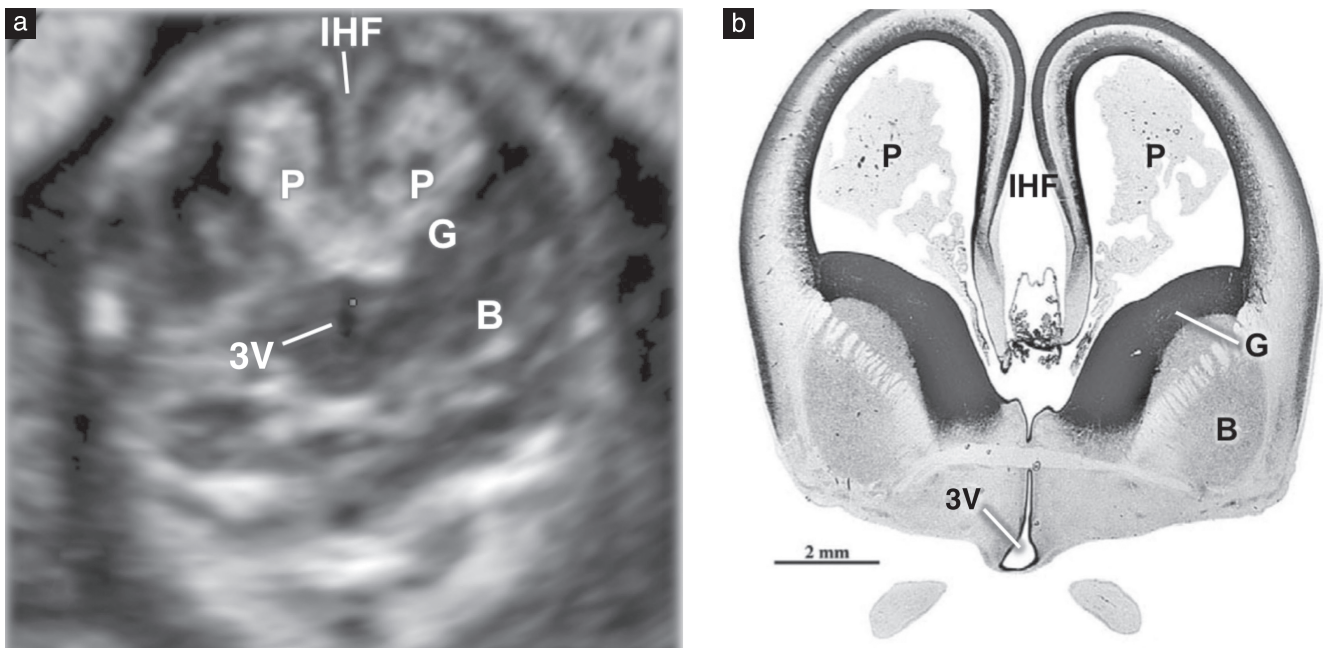


**Figure 7** Transcaudate coronal view of normal fetal brain, showing: (a) detailed anatomy on two-dimensional ultrasound imaging at 11–13 weeks and (b) corresponding anatomic specimen. 3V, third ventricle; B, basal ganglion; G, ganglionic eminence; IHF, interhemispheric fissure; P, choroid plexus of lateral ventricle. Anatomic specimen reproduced from Bayer and Altman<sup>16</sup> with permission.

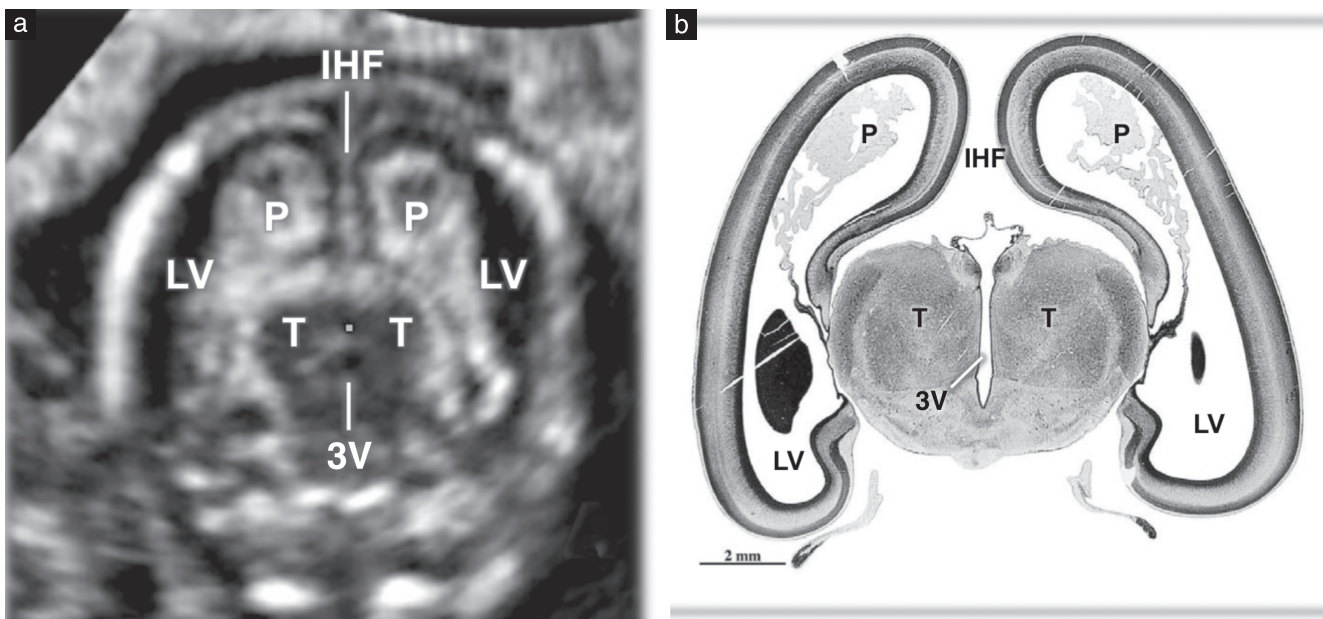


**Figure 8** Transthalamic coronal view of normal fetal brain, showing: (a) detailed anatomy on two-dimensional ultrasound imaging at 11–13 weeks and (b) corresponding anatomic specimen. 3V, third ventricle; IHF, interhemispheric fissure; LV, lateral ventricle; P, choroid plexus; T, thalamus. Anatomic specimen reproduced from Bayer and Altman<sup>16</sup> with permission.

more anterior one, passing through the pons and medulla (Figure 9), and a more posterior one, including the 4V and the medulla below it (Figure 10).

**Vascular anatomy at 11–13 weeks**

Thanks to the use of new, highly sensitive Doppler technology, visualization of the main fetal cerebral vessels is also feasible at 11–13 weeks<sup>30,31</sup>. In the sagittal views (Figure 11), it is possible to display the pericallosal arteries

with their branches, and the internal carotid artery below them. A few venous structures are also visible, such as the superior sagittal sinus underneath the calvarium, the straight sinus at the level of the cerebellar tentorium, continuing into the vein of Galen anteriorly, and joining the straight sinus into the torcular herophili, posteriorly. In the axial views, Doppler imaging allows visualization of the circle of Willis, including anterior, middle and posterior cerebral arteries (Figure 12).

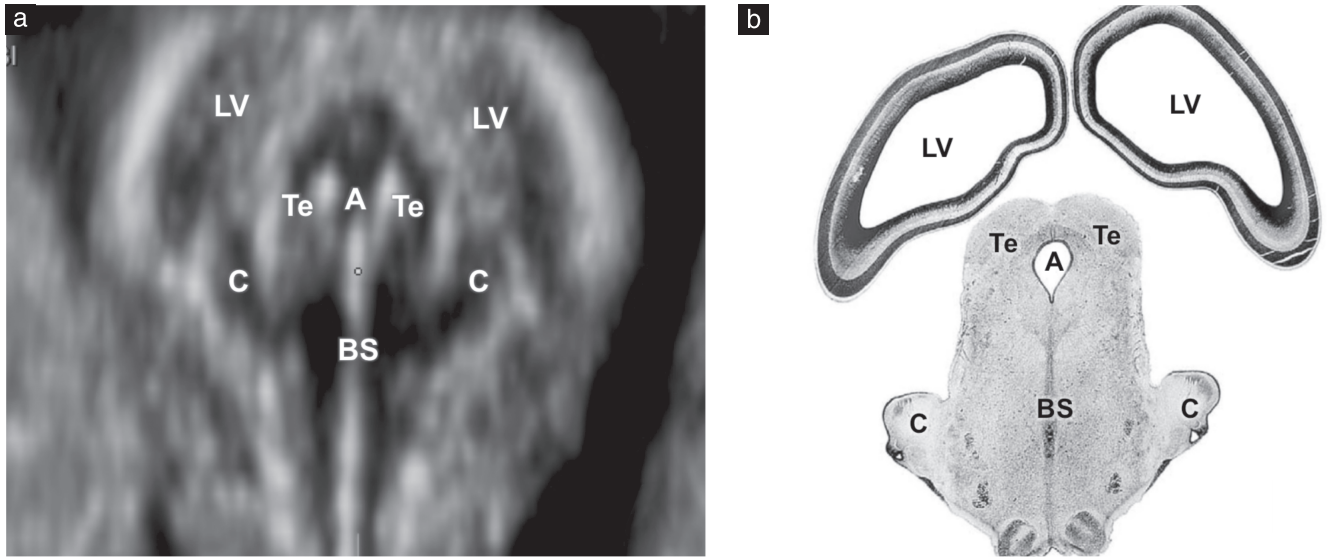


**Figure 9** Occipital coronal view of normal fetal brain, anterior to fourth ventricle, showing: (a) detailed anatomy on two-dimensional ultrasound imaging at 11–13 weeks and (b) corresponding anatomic specimen. A, aqueduct of Sylvius; BS, brainstem (pons and medulla); C, future cerebellar hemisphere; LV, lateral ventricle; Te, tectum. Anatomic specimen reproduced from Bayer and Altman<sup>16</sup> with permission.

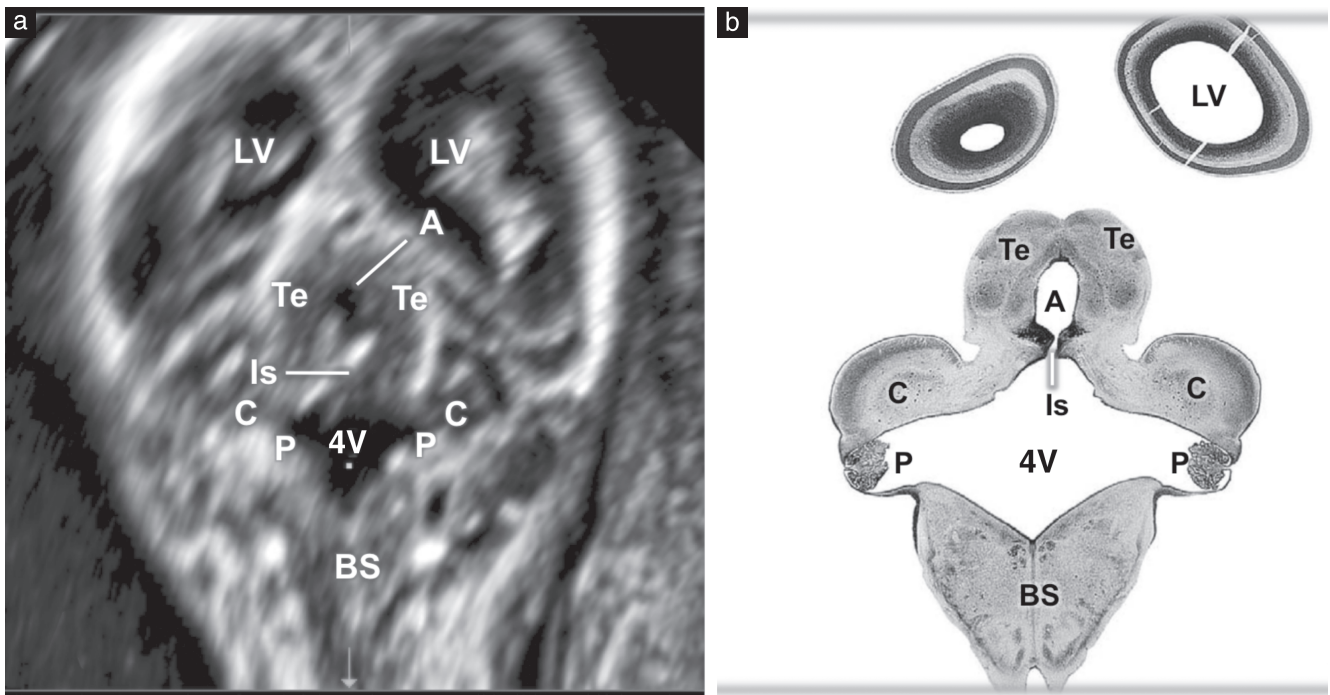


**Figure 10** Occipital coronal view of normal fetal brain, at level of fourth ventricle, showing: (a) detailed anatomy on two-dimensional ultrasound imaging at 11–13 weeks and (b) corresponding anatomic specimen. 4V, fourth ventricle; A, aqueduct of Sylvius; BS, brainstem (pons and medulla); C, future cerebellar hemisphere; Is, isthmus; LV, lateral ventricle; P, rhombencephalic (fourth ventricle) choroid plexus; Te, tectum. Anatomic specimen reproduced from Bayer and Altman<sup>16</sup> with permission.

## ANOMALIES POTENTIALLY DETECTABLE BY FIRST-TRIMESTER EXPERT NEUROSONOGRAPHY

CNS abnormalities involving the structures included in a basic ultrasound examination are often identified early in gestation. High detection rates of acrania, encephalocele and alobar holoprosencephaly have been reported for the basic ultrasound examination<sup>6,7,12,17–19</sup>. However, an expert evaluation may allow early recognition of other major CNS anomalies, such as ventriculomegaly, open spina bifida (OSB), Dandy–Walker malformation and agenesis of the corpus callosum.

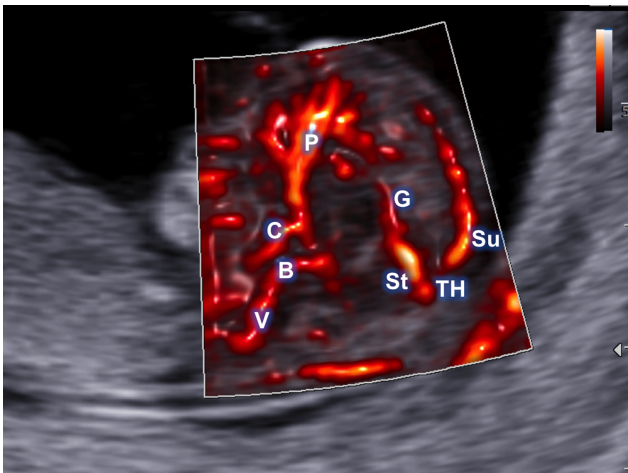


**Figure 11** Sagittal view of normal fetal brain using highly sensitive Doppler imaging (MV flow) at 11–13 weeks. B, basilar artery; C, internal carotid artery; G, vein of Galen; P, pericallosal artery; St, straight sinus; Su, superior sagittal sinus; TH, torcular herophili; V, vertebral artery.

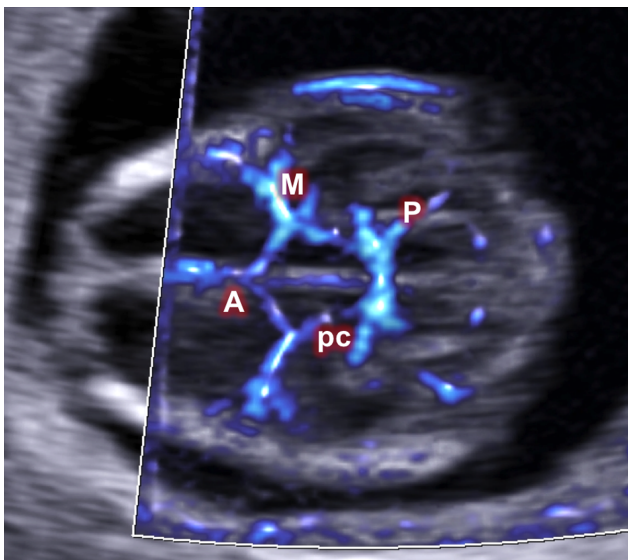


**Figure 12** Axial view of normal fetal brain showing circle of Willis using highly sensitive Doppler imaging (MV flow) at 11–13 weeks. A, anterior cerebral artery; M, middle cerebral artery; P, posterior cerebral artery; pc, posterior communicating artery.

## Ventriculomegaly

While the conventional definition of ventriculomegaly in the second trimester is an atrial diameter  $\geq 10$  mm, the diagnosis of this condition in the first trimester is not based on ventricular width. At the end of the first trimester, if the fluid content of a lateral ventricle is increased, it is a relative reduction of choroid plexus size, rather than an enlargement of the ventricle, that is noted<sup>32,33</sup> (Figure 13). It has been shown that a reduced ratio between the choroid plexus and ventricular areas may herald the diagnosis of ventriculomegaly according to its traditional definition on second-trimester ultrasound<sup>32,33</sup>. Specifically, at 11–13 weeks, ratios  $< 5^{\text{th}}$  percentile between the areas

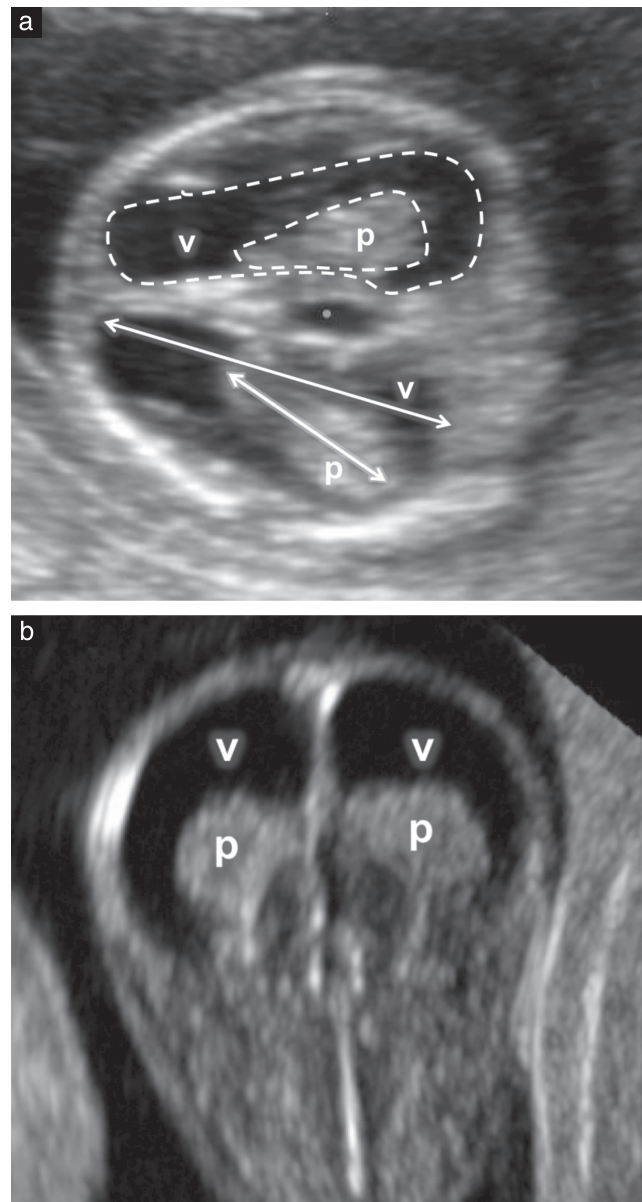


**Figure 13** Ventriculomegaly in first trimester. (a) In axial suprathalamic plane, ratios between lengths (arrows) and areas (dotted lines) of choroid plexus (p) and lateral ventricle (v) are reduced. (b) In coronal transthalamic view, neither choroid plexus reaches roof of corresponding lateral ventricle.

(5<sup>th</sup> percentile, 0.48–0.36), the lengths (5<sup>th</sup> percentile, 0.66–0.56) and the widths (5<sup>th</sup> percentile, 0.60–0.54) of these two structures have been reported to predict the diagnosis of ventriculomegaly in the mid trimester in 94%, 94% and 82% of cases, respectively<sup>32</sup>. It is therefore possible to establish a tentative diagnosis of cerebral ventriculomegaly in the first trimester, based on these ratios, although the available evidence is still limited. According to some, regardless of any quantitative measurement, the qualitative observation of hypoplastic choroid plexuses, i.e. being too small to reach the roof of the ventricles, should raise suspicion of early-onset ventriculomegaly<sup>34</sup> (Figure 13).

### Open spina bifida (OSB)

An abnormal appearance of the CPF in the mid-trimester has been shown to be associated with OSB in the majority of cases<sup>23,24,35,36</sup>. Recent studies have demonstrated that early indirect cranial findings of OSB can be noted in the midsagittal view in the first trimester, when direct visualization of the spinal defect may be challenging. Among fetuses affected by Chiari-II malformation, a reduced width of the CM can be demonstrated. In the frontal midsagittal view, instead of the three parallel anechoic spaces described above (BS, 4V/intracranial translucency and CM, Figure 3), the dominance of the BS, combined with a thinning of the 4V and CM and/or an absence of separation between them, have been described as fair predictors of OSB<sup>23,24,35,36</sup>. It has been determined that, due to the caudal displacement of the BS and 4V, the CM is collapsed and therefore not visible sonographically in the majority of these cases (Figure 14).

Some recent studies have proposed quantifying the anteroposterior diameter ratios between the three CPF structures visible in the midsagittal view, in order

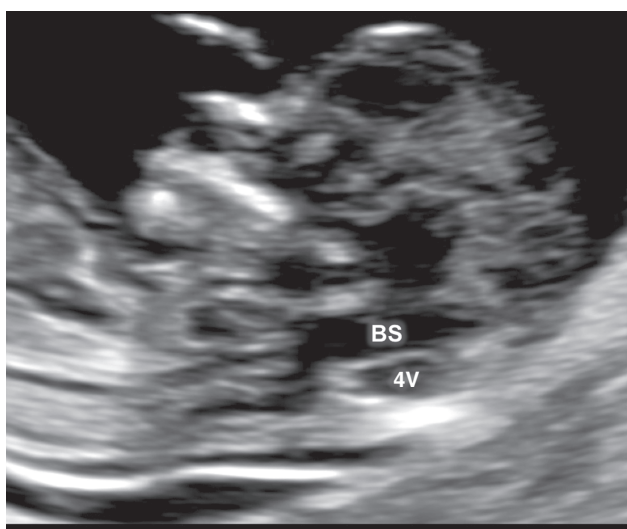


**Figure 14** Appearance of Chiari-II malformation in midsagittal view in first trimester. Brainstem (BS) is thicker than usual and displaced posteriorly, compressing fourth ventricle (4V), with consequent collapse of cisterna magna.

to demonstrate objectively Chiari-II malformation and to predict the presence of OSB. It has been proven that an increased ratio between BS thickness and its distance from the occipital bone (BS-to-occipital bone distance (BSOB), Figure 3) is a reliable and reproducible sonographic marker of OSB. Specifically, a BS/BSOB ratio > 95<sup>th</sup> percentile between 11 + 0 and 13 + 6 weeks has been found to predict almost all cases of OSB<sup>24,25,37</sup>, performing better than does qualitative assessment or measurement individually of every structure of the CPF, including the BS, BSOB and intracranial translucency.

In axial views also, the presence of abnormal brain findings in fetuses with OSB has been reported at 11–13 weeks of gestation. Due to leakage of fluid through the foramen magnum, in the case of Chiari-II anomaly, the amount of fluid in the ventricular system is reduced; the sonographic appearance of this has been described as ‘dry brain’<sup>38,39</sup> (Figure 15), with the third ventricle and the aqueduct of Sylvius barely visible. Moreover, the sonographic appearance as a result of the displacement backwards of the mid-brain and aqueduct, which are pushed closer to the occipital bone, known as ‘crash sign’ (Figure 15), has been found to herald the presence of OSB in the majority of cases and seems to reflect the early changes in shape of the BS in fetuses with Chiari-II anomaly<sup>40,41</sup>. Some authors have proposed quantifying in the axial plane the proximity of the aqueduct to the occipital bone, reporting a significant shortening of the distance between these two structures in cases of OSB<sup>42</sup>.

Recently, a multicenter case series compared the accuracy of all sonographic markers of OSB in both midsagittal and axial views of the fetal brain in the first trimester<sup>25</sup>. This study found the most accurate predictor of OSB to be the BS/BSOB ratio, with an area under the receiver-operating-characteristics curve of 0.997 and no cases of intact spine having a ratio > 1.

Since the CPF structures can be visualized exactly in the same scanning plane as that in which the NT is measured,



**Figure 15** Appearance of Chiari-II malformation in axial transthalamic view in first trimester. Third ventricle and aqueduct of Sylvius (arrow) are barely visible (‘dry brain’) and midbrain is displaced backwards, with aqueduct pushed close to occipital bone (‘crash sign’).



routine evaluation of the CPF seems feasible without much additional effort when performing routine screening for chromosomal abnormalities in the first trimester. This extended examination has been demonstrated to improve the early detection of OSB<sup>6,24,25,37</sup>. In a recent study, including a large population, it was shown that the detection rate of OSB improved from 15% to about 60% after implementing routine evaluation of the CPF structures in the anatomic protocol for the first-trimester ultrasound examination<sup>6</sup>.

### Dandy–Walker malformation (DWM)

Historically, sonographic diagnosis of cystic CPF anomalies and accurate differentiation between the classic DWM and the more common and benign Blake's pouch cyst (BPC) have been considered feasible only after 20 gestational weeks. In the last decade, first-trimester detection of CPF malformations by expert fetal brain scanning has been reported independently by several research groups<sup>27,29,36,43–48</sup>. In the frontal midsagittal plane, in fetuses with DWM or BPC, an increased amount of fluid in the 4V and CM, with fusion of these two structures, has been reported at 11–13 weeks<sup>36,43,47,48</sup>. Due to the wide communication between the 4V and CM, others have suggested that, in fetuses with cystic anomalies of the CPF, only two, rather than three, parallel anechoic spaces are visible in the midsagittal plane<sup>36,44,49</sup>. A reduced BS/BSOB ratio has been proposed as an early objective marker of cystic CPF anomaly; BS/BSOB < 5<sup>th</sup> percentile in the first trimester has been shown to predict the sonographic appearance of DWM or BPC at mid-gestation in a large proportion of cases, and to suggest a cystic CPF anomaly rather than OSB when only two parallel anechoic spaces are visible in the midsagittal plane<sup>36,43,49</sup> (Figure 16).

Upward displacement of the tentorium cerebelli with respect to its normal insertion on the occipital clivus is among the major criteria that differentiate DWM from BPC in fetuses with abnormal communication between the 4V and the CM. Although antenatal visualization

of the position of the tentorium cerebelli is technically challenging, especially in the first trimester, the torcular herophili, which lies at the intersection between the tentorium and the falx cerebri, may be depicted sonographically by means of highly sensitive Doppler imaging (Figure 11). On this basis, antenatal demonstration of the torcular herophili on Doppler imaging has been proposed as a proxy for the insertion of the tentorium on the fetal skull. Some recent studies have suggested that, thanks to visualization of the torcular herophili on first-trimester fetal neurosonography, the differential diagnosis between DWM and BPC may be feasible<sup>31</sup>. Volpe *et al.*<sup>31</sup> have shown that, in the frontal midsagittal view of the brain in fetuses with abnormal communication between the 4V and the CM, a very small angle between the BS and the tentorium (with the straight sinus appearing almost parallel to the BS) may predict the occurrence of DWM even in the first trimester<sup>31</sup>. Research by our group has shown that sonographic demonstration of the torcular herophili in the second trimester is feasible and may assist in the differential diagnosis between BPC and DWM<sup>50</sup>.

In fetuses with suspected CPF anomalies, a detailed sonographic study of the developing cerebellar vermis is feasible in the midsagittal plane only via the posterior fontanel. In this scanning plane, the vermis can be visualized and measured<sup>46</sup>. Moreover, additional quantitative and qualitative parameters have been proposed recently, such as the angle formed by the vermis and the pons (pontovermian angle) and the appearance of the aqueduct of Sylvius. It has been suggested, that among fetuses with CPF anomalies, the pontovermian angle is > 100°, being increased considerably in DWM and to a lesser extent in BPC<sup>29</sup>. Furthermore, in the first trimester, the aqueduct of Sylvius might appear smaller or larger than normal in case of DWM or BPC, respectively<sup>29</sup>.

### Agensis of the corpus callosum

In the midsagittal plane of the fetal head, the corpus callosum becomes detectable sonographically after

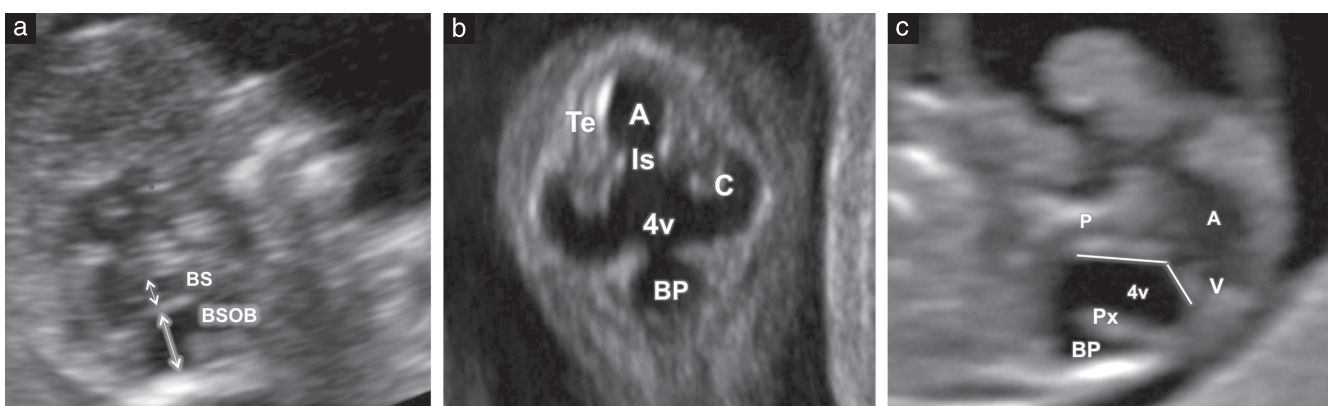


**Figure 16** Appearance of cystic anomaly of posterior fossa in first trimester. In midsagittal view (a), ratio between brainstem (BS) thickness and BS-to-occipital bone distance (BSOB) is reduced and only two rather than three parallel anechoic spaces are seen. In occipital coronal view (b), fourth ventricle (4v) appears enlarged, with prominence of aqueduct of Sylvius (A) and Blake's pouch (BP). (c) In midsagittal view, pontovermian angle is increased. C, future cerebellar hemisphere; Is, isthmus; P, pons; Px, plexus of fourth ventricle; Te, tectum; V, vermis.

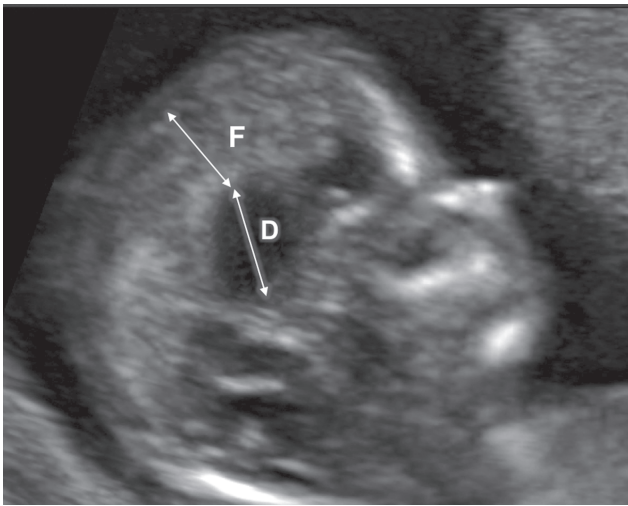


**Figure 17** Agenesis of corpus callosum in midsagittal view in first trimester, showing increased ratio between diencephalon (D) and falx (F) diameters.

16–18 weeks<sup>51,52</sup>. In the first trimester it is therefore not possible to suspect callosal agenesis based on the lack of its direct visualization on grayscale ultrasound imaging. However, some authors have proposed seeking indirect signs of callosal absence at 11–13 weeks. In 80% of fetuses that had agenesis of the corpus callosum diagnosed later in gestation, Lachmann *et al.*<sup>53</sup> demonstrated an increased ratio between the diencephalon diameter (from midbrain to falx, including third ventricle and thalami) and the falx diameter (Figure 17). This sonographic marker seems to reflect early in gestation the upward displacement and dilatation of the third ventricle, which is commonly noted in the midtrimester in fetuses with absent corpus callosum.

Several groups, independently, have used 2D and 3D power Doppler ultrasound to evaluate the presence and course of the pericallosal arteries in the first trimester. It was demonstrated that visualization of a normal artery was associated with the later appearance of a normal corpus callosum in all cases, whereas callosal agenesis was diagnosed in the midtrimester when the artery was not demonstrated in the first trimester<sup>30,54,55</sup>. In accordance with this finding, sonographic visualization of the pericallosal artery was suggested as an indirect but reliable sign to rule out callosal agenesis on first-trimester neurosonography.

## CONCLUSION

In conclusion, in the axial planes, a ‘basic’ examination of the fetal brain may be performed in accordance with current ISUOG guidelines for first-trimester ultrasound examination. However, using this approach, only the most severe or lethal brain abnormalities can be picked up sonographically at 11–13 weeks. With inclusion of non-axial planes, multiplanar neurosonography may be carried out at the end of the first trimester, following the methodology recommended for dedicated fetal brain

scanning in the midtrimester. Expert neurosonography with two- and three-dimensional imaging in the first trimester, combined with detailed knowledge of fetal anatomy and sonoembryology, allows detection of early signs of several brain abnormalities which are commonly diagnosed only later in gestation and whose early diagnosis can be clinically advantageous. This detailed examination of the CNS can be offered to parents at high risk for fetal anomalies based on the family history or on the presence of abnormal findings during the basic ultrasound examination. A standardized protocol for first-trimester neurosonography at 11–13 weeks, including systematic evaluation of specific markers for structural abnormalities (such as the BS/BSOB ratio), is expected to detect or predict the development of most severe brain anomalies.

## ACKNOWLEDGMENT

We acknowledge the contribution of Dr Paolo Volpe, whose commitment and research activity on expert assessment of the fetal anatomy in the first trimester inspired the design of this work.

## REFERENCES

- Morris JK, Wellesley DG, Barisic I, Addor MC, Bergman JEH, Braz P, Cavero-Carbonell C, Draper ES, Gatt M, Haeusler M, Klungsoyr K, Kurinczuk JJ, Lelong N, Luyt K, Lynch C, O'Mahony MT, Mokoroa O, Nelen V, Neville AJ, Pierini A, Randrianaivo H, Rankin J, Rissmann A, Rouget F, Schaub B, Tucker DF, Verellen-Dumoulin C, Wiesel A, Zymak-Zakutnia N, Lanzoni M, Garne E. Epidemiology of congenital cerebral anomalies in Europe: A multicentre, population-based EUROCAT study. *Arch Dis Child* 2019; 104: 1181–1187.
- Anderson N, Boswell O, Duff G. Prenatal sonography for the detection of fetal anomalies: Results of a prospective study and comparison with prior series. *Am J Roentgenol* 1995; 165: 943–950.
- Bernaschek G, Stuempflen I, Deutinger J. The value of sonographic diagnosis of fetal malformations: Different results between indication-based and screening-based investigations. *Prenat Diagn* 1994; 14: 807–812.
- International Society of Ultrasound in Obstetrics & Gynecology Education Committee. Sonographic examination of the fetal central nervous system: guidelines for performing the ‘basic examination’ and the ‘fetal neurosonogram’. *Ultrasound Obstet Gynecol* 2007; 29: 109–116.
- Syngelaki A, Chelemen T, Dagklis T, Allan L, Nicolaidis KH. Challenges in the diagnosis of fetal non-chromosomal abnormalities at 11–13 weeks. *Prenat Diagn* 2011; 31: 90–102.
- Syngelaki A, Hammami A, Bower S, Zidere V, Akolekar R, Nicolaidis KH. Diagnosis of fetal non-chromosomal abnormalities on routine ultrasound examination at 11–13 weeks’ gestation. *Ultrasound Obstet Gynecol* 2019; 54: 468–476.
- Rossi AC, Prefumo F. Accuracy of ultrasonography at 11–14 weeks of gestation for detection of fetal structural anomalies: A systematic review. *Obstet Gynecol* 2013; 122: 1160–1167.
- Rayburn WF, Jolley JA, Simpson LL. Advances in ultrasound imaging for congenital malformations during early gestation. *Birth Defects Res A Clin Mol Teratol* 2015; 103: 260–268.
- Iliescu D, Tudorache S, Comanescu A, Antsaklis P, Cotarcea S, Novac L, Cernea N, Antsaklis A. Improved detection rate of structural abnormalities in the first trimester using an extended examination protocol. *Ultrasound Obstet Gynecol* 2013; 42: 300–309.
- Grande M, Arigita M, Borobio V, Jimenez JM, Fernandez S, Borrell A. First-trimester detection of structural abnormalities and the role of aneuploidy markers. *Ultrasound Obstet Gynecol* 2012; 39: 157–163.
- Bardi F, Smith E, Kuilman M, Snijders RJM, Bilardo CM. Early Detection of Structural Anomalies in a Primary Care Setting in the Netherlands. *Fetal Diagn Ther* 2019; 46: 12–19.
- Karim JN, Roberts NW, Salomon LJ, Papageorghiou AT. Systematic review of first-trimester ultrasound screening for detection of fetal structural anomalies and factors that affect screening performance. *Ultrasound Obstet Gynecol* 2017; 50: 429–441.
- Vayna AM, Veduta A, Duta S, Panaitescu AM, Stoica S, Buinoiu N, Nedelea F, Peltecu G. Diagnosis of fetal structural anomalies at 11 to 14 weeks. *J Ultrasound Med* 2018; 37: 2063–2073.
- Kenkhuys MJA, Bakker M, Bardi F, Fontanella F, Bakker MK, Fleurke-Rozema JH, Bilardo CM. Effectiveness of 12–13-week scan for early diagnosis of fetal

- congenital anomalies in the cell-free DNA era. *Ultrasound Obstet Gynecol* 2018; 51: 463–469.
15. Salomon LJ, Alfirevic Z, Bilardo CM, Chalouhi GE, Ghi T, Kagan KO, Lau TK, Papageorgiou AT, Raine-Fenning NJ, Stirrenemann J, Suresh S, Tabor A, Timor-Tritsch IE, Toi A, Yeo G. ISUOG Practice Guidelines: performance of first-trimester fetal ultrasound scan. *Ultrasound Obstet Gynecol* 2013; 41: 102–113.
  16. Bayer S, Altman J. *The Human Brain During The Late First Trimester. Atlas of Human Central Nervous System Development, Volume 4*. CRC Press: Boca Raton, 2006.
  17. Sepulveda W, Wong AE, Andreeva E, Odegova N, Martinez-Ten P, Meagher S. Sonographic spectrum of first-trimester fetal cephalocele: Review of 35 cases. *Ultrasound Obstet Gynecol* 2015; 46: 29–33.
  18. Cheng CC, Lee FK, Lin HW, Shih JC, Tsai MS. Diagnosis of fetal acrania during the first trimester nuchal translucency screening for Down syndrome. *Int J Gynecol Obstet* 2003; 80: 139–144.
  19. Sepulveda W, Wong AE. First trimester screening for holoprosencephaly with choroid plexus morphology (“butterfly” sign) and biparietal diameter. *Prenat Diagn* 2013; 33: 1233–1237.
  20. Nicolaides KH, Azar G, Byrne D, Mansur C, Marks K. Fetal nuchal translucency: Ultrasonographic screening for chromosomal defects in first trimester of pregnancy. *Br Med J* 1992; 304: 867–869.
  21. Nicolaides KH, Brizot ML, Sniijders RJM. Fetal nuchal translucency: ultrasound screening for fetal trisomy in the first trimester of pregnancy. *ACOG Curr J Rev* 1995; 8: 42.
  22. Nicolaides KH, Heath V, Cicero S. Increased fetal nuchal translucency at 11–14 weeks. *Prenat Diagn* 2002; 22: 308–315.
  23. Chaoui R, Benoit B, Mitkowska-Wozniak H, Heling KS, Nicolaides KH. Assessment of intracranial translucency (IT) in the detection of spina bifida at the 11–13-week scan. *Ultrasound Obstet Gynecol* 2009; 34: 249–252.
  24. Lachmann R, Chaoui R, Moratalla J, Picciarelli G, Nicolaides KH. Posterior brain in fetuses with open spina bifida at 11 to 13 weeks. *Prenat Diagn* 2011; 31: 103–106.
  25. Wertaschnigg D, Ramkrishna J, Ganesan S, Tse C, Scheier M, Volpe N, Ghi T, Meagher S, Rolnik DL. Cranial sonographic markers of fetal open spina bifida at 11 to 13 weeks of gestation. *Prenat Diagn* 2020; 40: 365–372.
  26. Robinson AJ. Inferior vermian hypoplasia - Preconception, misconception. *Ultrasound Obstet Gynecol* 2014; 43: 123–136.
  27. Robinson AJ, Goldstein R. The cisterna magna septa: Vestigial remnants of Blake's pouch and a potential new marker for normal development of the rhombencephalon. *J Ultrasound Med* 2007; 26: 83–95.
  28. Altmann R, Scharnreiter I, Scheier T, Mayer R, Arzt W, Scheier M. Sonoembryology of the fetal posterior fossa at 11 + 3 to 13 + 6 gestational weeks on three-dimensional transvaginal ultrasound. *Prenat Diagn* 2016; 36: 731–737.
  29. Paladini D, Donarini G, Parodi S, Chaoui R. Differentiating features of posterior fossa at 12–13 weeks' gestation in fetuses with Dandy–Walker malformation and Blake's pouch cyst. *Ultrasound Obstet Gynecol* 2019; 53: 850–852.
  30. Conturso R, Contro E, Bellussi F, Youssef A, Pacella G, Martelli F, Rizzo N, Pilu G, Ghi T. Demonstration of the pericallosal artery at 11–13 weeks of gestation using 3D ultrasound. *Fetal Diagn Ther* 2015; 37: 305–309.
  31. Volpe P, Persico N, Fanelli T, De Robertis V, D'Alessandro J, Boito S, Pilu G, Votino C. Prospective detection and differential diagnosis of cystic posterior fossa anomalies by assessing posterior brain at 11–14 weeks. *Am J Obstet Gynecol MFM* [Internet]. 2019; 1: 173–181. <https://doi.org/10.1016/j.ajogmf.2019.06.004>.
  32. Manegold-Brauer G, Oseledchik A, Floeck A, Berg C, Gembruch U, Geipel A. Approach to the sonographic evaluation of fetal ventriculomegaly at 11 to 14 weeks gestation. *BMC Pregnancy Childbirth* [Internet]. 2016; 16: 1–8. <http://dx.doi.org/10.1186/s12884-016-0797-z>.
  33. Loureiro T, Ushakov F, Maiz N, Montenegro N, Nicolaides KH. Lateral ventricles in fetuses with aneuploidies at 11–13 weeks' gestation. *Ultrasound Obstet Gynecol* 2012; 40: 282–287.
  34. Ushakov F, Chitty LS. P30.03: Ventriculomegaly at 11–14 weeks: diagnostic criteria and outcome. *Ultrasound Obstet Gynecol* 2016; 48 (Suppl): 267.
  35. Chaoui R, Nicolaides KH. From nuchal translucency to intracranial translucency: Towards the early detection of spina bifida. *Ultrasound Obstet Gynecol* 2010; 35: 133–138.
  36. Martinez-Ten P, Illescas T, Adiego B, Estevez M, Bermejo C, Wong AE, Sepulveda W. Non-visualization of choroid plexus of fourth ventricle as first-trimester predictor of posterior fossa anomalies and chromosomal defects. *Ultrasound Obstet Gynecol* 2018; 51: 199–207.
  37. Chaoui R, Benoit B, Heling KS, Kagan KO, Pietzsch V, Sarut Lopez A, Tekesin I, Karl K. Prospective detection of open spina bifida at 11–13 weeks by assessing intracranial translucency and posterior brain. *Ultrasound Obstet Gynecol* 2011; 38: 722–726.
  38. Loureiro T, Ushakov F, Montenegro N, Gielchinsky Y, Nicolaides KH. Cerebral ventricular system in fetuses with open spina bifida at 11–13 weeks' gestation. *Ultrasound Obstet Gynecol* 2012; 39: 620–624.
  39. Chaoui R, Benoit B, Entezami M, Frenzel W, Heling KS, Ladendorf B, Pietzsch V, Sarut Lopez A, Karl K. Ratio of fetal choroid plexus to head size: simple sonographic marker of open spina bifida at 11–13 weeks' gestation. *Ultrasound Obstet Gynecol* 2020; 55: 81–86.
  40. Ushakov F, Sacco A, Andreeva E, Tudorache S, Everett T, David AL, Pandya PP. Crash sign: new first-trimester sonographic marker of spina bifida. *Ultrasound Obstet Gynecol* 2019; 54: 740–745.
  41. Chaoui R, Nicolaides KH. Detecting open spina bifida at the 11–13-week scan by assessing intracranial translucency and the posterior brain region: mid-sagittal or axial plane? *Ultrasound Obstet Gynecol* 2011; 38: 609–612.
  42. Finn M, Sutton D, Atkinson S, Ransome K, Sujenthiran P, Ditcham V, Wakefield P, Meagher S. The aqueduct of Sylvius: A sonographic landmark for neural tube defects in the first trimester. *Ultrasound Obstet Gynecol* 2011; 38: 640–645.
  43. Lachmann R, Sinkovskaya E, Abuhamad A. Posterior brain in fetuses with Dandy-Walker malformation with complete agenesis of the cerebellar vermis at 11–13 weeks: A pilot study. *Prenat Diagn* 2012; 32: 765–769.
  44. Volpe P, Contro E, Fanelli T, Muto B, Pilu G, Gentile M. Appearance of fetal posterior fossa at 11–14 weeks in fetuses with Dandy-Walker malformation or chromosomal anomalies. *Ultrasound Obstet Gynecol* 2016; 47: 720–725.
  45. Iuculano A, Zoppi MA, Ibba RM, Monni G. A Case of Enlarged Intracranial Translucency in a Fetus with Blake's Pouch Cyst. *Case Rep Obstet Gynecol* 2014; 2014: 968089.
  46. Altmann R, Schertler C, Scharnreiter I, Arzt W, Dertinger S, Scheier M. Diagnosis of Fetal Posterior Fossa Malformations in High-Risk Pregnancies at 12–14 Gestational Weeks by Transvaginal Ultrasound Examination. *Fetal Diagn Ther* 2020; 47: 182–187.
  47. Lafouge A, Gorincour G, Desbriere R, Quarello E. Prenatal diagnosis of Blake's pouch cyst following first-trimester observation of enlarged intracranial translucency. *Ultrasound Obstet Gynecol* 2012; 40: 479–480.
  48. Garcia-Posada R, Eixarch E, Sanz M, Puerto B, Figueras F, Borrell A. Cisterna magna width at 11–13 weeks in the detection of posterior fossa anomalies. *Ultrasound Obstet Gynecol* 2013; 41: 515–520.
  49. Volpe P, Muto B, Passamonti U, Rembouskos G, De Robertis V, Campobasso G, Tempesta A, Volpe G, Fanelli T. Abnormal sonographic appearance of posterior brain at 11–14 weeks and fetal outcome. *Prenat Diagn* 2015; 35: 717–723.
  50. Dall'Asta A, Grisolia G, Volpe N, Schera GBL, Sorrentino F, Frusca T. Prenatal visualization of the torcular herophili by means of a Doppler technology highly sensitive for low velocity flow in the expert assessment of the posterior fossa: a prospective study. *BJOG* 2020. DOI:10.1111/1471-0528.16392.
  51. Malinge G, Zakut H. The corpus callosum: normal fetal development as shown by transvaginal sonography. *Am J Roentgenol* 1993; 161: 1041–1043.
  52. Achiron R, Achiron A. Development of the human fetal corpus callosum: a high-resolution, cross-sectional sonographic study. *Ultrasound Obstet Gynecol* 2001; 18: 343–347.
  53. Lachmann R, Sodre D, Barmpas M, Akolekar R, Nicolaides KH. Midbrain and falx in fetuses with absent corpus callosum at 11–13 weeks. *Fetal Diagn Ther* 2013; 33: 41–46.
  54. Pati M, Cani C, Bertucci E, Re C, Latella S, D'Amico R, Mazza V. Early visualization and measurement of the pericallosal artery: An indirect sign of corpus callosum development. *J Ultrasound Med* 2012; 31: 231–237.
  55. Diaz-Guerrero L, Giugni-Chalbaud G, Sosa-Olavarria A. Assessment of pericallosal arteries by color Doppler ultrasonography at 11–14 weeks: An early marker of fetal corpus callosum development in normal fetuses and agenesis in cases with chromosomal anomalies. *Fetal Diagn Ther* 2013; 34: 85–89.